The Journal of Experimental Biology 207, 3657-3665
Published by The Company of Biologists 2004
doi:10.1242/jeb.01207

Structural and functional imaging of bottlenose dolphin (*Tursiops truncatus*) cranial anatomy

Dorian S. Houser[1], James Finneran[2], Don Carder[2], William Van Bonn[2], Cynthia Smith[2], Carl Hoh[3], Robert Mattrey[3] and Sam Ridgway[2,3,*]

[1]*BIOMIMETICA, La Mesa, CA 91942, USA,* [2]*Space and Naval Warfare Systems Center, San Diego, CA 92152, USA* and [3]*School of Medicine, University of California, San Diego, CA 92103, USA*

*Author for correspondence (e-mail: ridgway@spawar.navy.mil)

Accepted 22 July 2004

Summary

Bottlenose dolphins were submitted to structural (CT) and functional (SPECT/PET) scans to investigate their *in vivo* anatomy and physiology with respect to structures important to hearing and echolocation. The spatial arrangement of the nasal passage and sinus air spaces to the auditory bullae and phonic lips was studied in two dolphins *via* CT. Air volume of the sinuses and nasal passages ranged from 267.4 to 380.9 ml. Relationships of air spaces to the auditory bullae and phonic lips support previous hypotheses that air protects the ears from echolocation clicks generated by the dolphin and contributes to dolphin hearing capabilities (e.g. minimum angular resolution, inter-aural intensity differences). Lung air may replenish reductions in sinus and nasal passage air volume *via* the palatopharyngeal sphincter, thus permitting the echolocation mechanism to operate at depth. To determine the relative extent of regional blood flow within the head of the dolphin, two dolphins were scanned with SPECT after an intravenous dose of 1850 MBq ^{99m}Tc-bicisate. A single dolphin received 740 MBq of ^{18}F-2-fluoro-2-deoxyglucose (FDG) to identify the relative metabolic activity of head tissues. Substantial blood flow was noted across the dorsoanterior curvature of the melon and within the posterior region of the lower jaw fats. Metabolism of these tissues relative to others within the head was nominal. It is suggested that blood flow in these fat bodies serves to thermoregulate lipid density of the melon and jaw canal. Sound velocity is inversely related to the temperature of acoustic lipids (decreasing lipid density), and changes in lipid temperature are likely to impact the wave guide properties of the sound projection and reception pathways. Thermoregulation of lipid density may maintain sound velocity gradients of the acoustic lipid complexes, particularly in the outer shell of the melon, which otherwise might vary in response to changing environmental temperatures.

Key words: CT, PET, SPECT, scan, cranium, hearing, echolocation, lipid density, bottlenose dolphin, *Tursiops truncatus.*

Introduction

Decades of psychoacoustic and physiological experimentation and *postmortem* analyses of dolphin cranial anatomy have resulted in our current understanding of the acoustics and biomechanics of dolphin echolocation. Psychoacoustic experimentation, in particular, has characterized not only the physics of echolocation (e.g. echolocation pulse length, source levels, transmit beams) but has also identified the detection and discrimination capabilities that it imparts to the dolphin (Au, 1993). Hearing sensitivity, frequency and amplitude discrimination have also been discerned *via* psychoacoustic means, providing additional characterization of auditory system function (Nachtigall et al., 2000). Physiological experimentation coupled with anatomical investigation has revealed mechanisms of sound production in the nasal system (Dormer, 1974; Ridgway et al., 1980) and sound conduction to the dolphin ear (Bullock and Ridgway, 1972; McCormick et al., 1970). *Postmortem* anatomical investigations have been crucial to inferring the role of specific anatomical structures to sound production and reception processes (Cranford, 2000; Ketten, 2000), but establishing definitive quantitative and qualitative relationships between structure and function has been a difficult task. It remains a substantial impediment to a comprehensive understanding of the biomechanics of delphinid sound production and reception.

Reports on the *postmortem* investigation of delphinid anatomy date back to the 18th century (Hunter, 1787), with more comprehensive, multi-species reports on cetacean cranial anatomy surfacing during the past century (e.g. Fraser and Purves, 1960). These *postmortem* studies have revealed numerous anatomical variations on the terrestrial mammal theme that are important to sound generation and sound reception in an aquatic environment. In delphinids, the fusion

Table 1. *Age and physical attributes of subjects used in structural and functional imaging scans*

Animal I.D.	Sex	Age (years)	Mass (kg)	Length (cm)	Scan type
CIN	F	22	122	222	CT
WEN	M	20	194	252	CT, SPECT, PET
FLP	M	25	212	256	CT, SPECT

of middle and inner ear into the tympano-periotic complex, the migration of the bullar complex from the skull, the presence of air sinuses around the bulla (Dudok van Heel, 1962; Fraser and Purves, 1960; Ketten, 2000), the presence of phonic lips (Cranford, 2000; Evans and Prescott, 1962), an isovaleric-rich fat body in the forehead known as the melon (Varanasi et al., 1975; Varanasi and Malins, 1971) and hollow lower jaws filled with acoustic lipids (Varanasi and Malins, 1970a,b) are a few notable adaptations favoring effective sound utilization in the ocean. The functional role of these adaptations has been inferred by assessing the spatial and structural relationship between anatomic components of the auditory and phonation system (e.g. Cranford et al., 1996), variation in design relative to terrestrial species (e.g. Dudok van Heel, 1962; Norris, 1964; Reysenbach de Haan, 1956), the physiological response of the system following anatomical manipulation (McCormick et al., 1970) and the biochemical composition of pertinent structures (Varanasi et al., 1975). These inferences, considered in relation to the results of psychoacoustic experiments (e.g. Brill, 1991) and physiological responses to manipulation of the system, form the basis for our current understanding of delphinid hearing and phonation.

The availability of computed tomography (CT) and magnetic resonance imaging (MRI) devices has stimulated more investigation to determine relationships between anatomical structures within the cetacean head by allowing internal anatomy to be viewed without laborious anatomical dissection. These imaging modalities have been used with *postmortem* specimens to study the brain of the bottlenose dolphin (*Tursiops truncatus*) and the white whale (*Delphinapterus leucas*; Marino et al., 2001a,b,c) as well as the *in situ* auditory anatomy and sound-producing structures of several cetacean species (Cranford, 1988; Cranford et al., 1996; Ketten, 1994; Ketten and Wartzok, 1990). As with necropsy procedures, functional properties of tissues are inferred from their biochemical composition, morphology and relationship to other tissues. Unfortunately, *postmortem* specimens often have to be frozen and then thawed for scanning, and such freezing and thawing may produce tissue distortion and permit the draining of fluids into air cavities with the breakdown of cell membranes and fracturing of capillaries. Furthermore, changes that begin after death can produce changes in tissue density, gas bubble generation from bacteria, swelling, *rigor mortis* and other distortions (Mackay, 1966). Tissue changes following death may therefore lead to spurious conclusions about tissue function. *In vivo* measurements made with CT and MRI can address these issues since such measurements preclude cavity and tissue deformations and biochemical changes of tissues that follow death.

Functional information of auditory and sound production tissues may be obtained through the use of functional scanning techniques [e.g. single photon emission computed tomography (SPECT) and positron emission tomography (PET)]. By following the distribution of administered radiopharmaceuticals and radionuclides, these scanning techniques allow certain aspects of the physiology of a subject, its organs and tissues, to be observed. In conjunction with *in vivo* CT and/or MRI measurements, consideration of functional information can provide a more comprehensive understanding of tissue function and structure than can be achieved through *postmortem* analysis alone.

The current study presents the first CT scans of living bottlenose dolphins and demonstrates the utility of *in vivo* anatomical analyses. It also presents the first functional scanning of a bottlenose dolphin; both PET and SPECT scans are used to couple information about cranial blood flow and metabolism within the dolphin to anatomical information gained *via* CT imaging. Results of this study provide new insight into dolphin anatomy and physiology that are pertinent to understanding the role of certain anatomical features in both hearing and echolocation.

Materials and methods

Three bottlenose dolphins (*Tursiops truncatus* Montagu 1821), two males (WEN and FLP) and one female (CIN), were used in both structural (CT) and functional (SPECT and PET) scanning procedures (Table 1). All three animals were trained to cooperate in the experiments by sliding out of the water and onto a cushioned mat at the trainer's signal. Each animal was trained to remain still once on the mat. Rewards of fish were given by the trainers for animal cooperation in remaining still for all procedures. The animals were transported to the scanning facilities in a covered van and were accompanied by at least one attending veterinarian as well as the animal's trainers. Four to six additional experienced animal care assistants were also present at all times. On arrival at the scan facility, dolphins were transferred to a specially created, padded gurney for movement into the scanner room. All experiments were conducted in accordance with a protocol approved by the Institutional Animal Care and Use Committee of the Navy Marine Mammal Program, Space and Naval Warfare Systems Center, San Diego, CA, USA as well as the University of California, San Diego, CA, USA.

CT scanning

Two dolphins (CIN and WEN) were transported to Vital Imaging of La Jolla, located approximately 12 miles from their

holding enclosures in San Diego Bay. Each dolphin received 0.3–0.55 mg kg^{-1} of diazepam to reduce any anxiety attendant with the scan. X-ray CT was performed using an electron beam scanner (Imatron, San Francisco, CA, USA) to study the cranial morphology of the dolphin. Volume acquisition mode was used to image the entire head. With this mode, X-ray data are acquired helically by rotating an X-ray source [130 KeV (kilo-electron volts) at 600 MAS (mAmpSec)] collimated to 3 mm around the object at 100 ms per revolution. Multiple X-ray projections are then obtained over a 270° arc while the object is translated through the gantry at 25 mm s^{-1}. Each data set (projections acquired from a single revolution) is used to reconstruct a single cross-sectional image representing the internal organs located within a transverse plane that is slightly more than 3 mm thick. Because the object translated 2.5 mm per revolution, a series of 3 mm-thick images are then made available that are separated by 2.5 mm. The slight overlap was chosen to produce smooth three-dimensional (3-D) or multiplanar reconstructions of the imaged region. Image data were saved in DICOM format and stored to disk until processed.

SPECT

SPECT was used to monitor blood flow in the head tissues of two dolphins. The SPECT scanner utilizes a gamma camera to acquire gamma rays that are emitted from radiopharmaceuticals administered to a subject prior to scanning. Gamma ray photons can be mapped into a two-dimensional (2-D) space; however, a SPECT camera can acquire images from multiple angles around the patient so that a 3-D image of the activity can be reconstructed. Technetium (^{99m}Tc) bicisate is a radiopharmaceutical with a high first pass blood extraction and slow clearance in brain tissue. This property makes it useful in the mapping of blood flow since the relative image intensity in a region of brain tissue reflects the underlying blood flow to that region. ^{99m}Tc-bicisate is a common diagnostic radiopharmaceutical for vascular irregularities of the human brain.

Dolphins (WEN and FLP) were administered ^{99m}Tc-bicisate (Syncor International Inc., Pasadena, CA, USA) to determine the distribution of blood flow within the brain and other soft tissues of the head. Two hours prior to SPECT imaging, the dolphins received a 1850 MBq intravenous injection of ^{99m}Tc-bicisate. Subjects were placed quiescent in a quiet, darkened room for 15 min following injection and were then transported to the Department of Nuclear Medicine at the University of California, San Diego Medical Center. Images were acquired on an ADAC Forte SPECT camera (Milpitas, CA, USA) with the dolphins placed on a specially engineered bed, allowing them to be properly cooled with water. The imaging acquisition consisted of 30 s per stop for a total of 64 angled stops divided between the two imaging heads. This resulted in a total scan time of approximately 32 min. After image reconstruction, the images were converted to the DICOM 3.0 format.

PET

PET was used to estimate the relative metabolism of dolphin cranial tissues. The PET scanner uses a circular array of detectors to measure photons produced from positron-emitting radiopharmaceuticals that have been administered to a subject prior to scanning. As in SPECT imaging, 3-D images of radiopharmaceutical distributions can be generated where the intensity of the image represents the relative concentration of the radiopharmaceutical accumulated in the tissue. ^{18}F-2-fluoro-2-deoxyglucose (FDG) is an analog of glucose and is often used in PET scanning to estimate glucose uptake by tissues and is commonly used in the detection of cancerous tissues because of the relatively higher metabolic rate of cancerous tissue to non-cancerous tissue.

A single dolphin (WEN) was administered 740 MBq of FDG (Syncor International Inc.) by intravenous injection ~2 h prior to scanning to map the relative metabolic activity of tissues within the brain and other soft tissues of the head. As in the SPECT procedure, the animal was kept in a quiet, darkened room for 40 min post-injection of the ligand. The dolphin was then transported as outlined above to the Vital Imaging Facility in Sorrento Valley, CA, where the PET scan took place. Images were acquired on a Seimens HR+ PET scanner (Knoxville, TN, USA) with the dolphin on the same specially engineered bed used in the SPECT scan. A 15-min transmission scan was first acquired for attenuation correction. The emission scan consisted of eight frames of 4-min acquisitions to allow for any subject movement. This resulted in a total scan time of approximately 55 min. The images were converted from the ECAT 7.2 format to the DICOM 3.0 format for further processing.

Data processing

Data acquired from all of the imaging modalities were processed using Analyze 4.0/5.0, created by the Biomedical Imaging Resource of the Mayo Clinic (Robb, 1999; Robb and Barillot, 1989; Robb et al., 1989). All data were converted to AVW format (native Analyze format) and volumes made cubic (equivalent voxel dimensions) through the use of linear interpolation. A threshold was applied to data from the CT scans according to tissue density (represented by X-ray attenuation in Houndsfield units), and binary representations of isolated tissues were created and formed into object maps. Objects were created for the skull, brain, tympano-periotic complex, surface of the dolphin and air spaces of the sinus cavities, nasal passages and larynx. Spatial relationships between structures were observed by visualizing the objects while suppressing the display of non-objectified tissues. The volume of air contained in the sinuses and nasal passages was calculated by multiplying the voxel density of the sinus/nasal passage object by the calibrated voxel dimensions.

Data from the PET and SPECT scans were co-registered to CT images to localize regions of metabolically active tissues and regions of blood flow. Primary registration was accomplished through application of an automated surface-matching algorithm within Analyze. This algorithm was applied to filled binary objects created from extractions of the brain from both the structural and functional images. Co-registration was achieved by manually fine-tuning the resulting

transform matrix after application to the original PET/SPECT and CT image volumes collected from the same animal. PET and SPECT data were also mapped to 24-bit RGB data representations to facilitate visualization of the image volumes.

Results

CT

Fig. 1 demonstrates the spatial relationship between the skull and the sinus cavities, nasal passages and laryngeal airspace. Fig. 2 demonstrates the same relationship but includes the auditory bulla, brain and spinal cord and remaining soft tissues of the head. Note the external landmarks (i.e. eye, mouth slit and blowhole) for reference of the internal placement of structures imaged in Fig. 1. Skull asymmetry is evident, as the midline of the skull, defined from the rostral bifurcation of the upper jaw, passes through the right bony nasal passage (Fig. 1C,D). The nasal passages and vertex of the skull are shifted left of the midline, as is typical of odontocete species (Cranford et al., 1996). Most of the sinuses and nasal passageways are contiguous, although small discontinuous pockets of air were identified. The nasal passages form the major body of air within the cranium and, in combination with the contiguous sinus spaces, comprised an air volume of 267.4 ml in CIN (Fig. 3A) and 368.7 ml in WEN (Fig. 3B). The inclusion of distinct air spaces separately compartmentalized from the contiguous air space, but excluding laryngeal air, increased the cranial air volume to 290.3 ml and 380.9 ml, respectively.

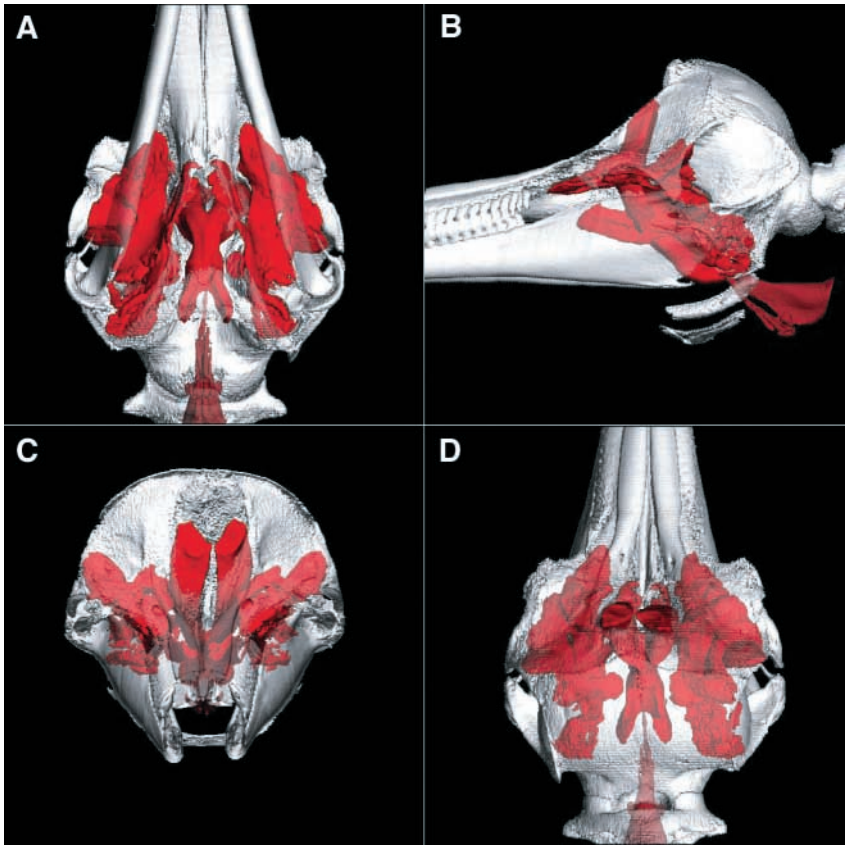

Fig. 1. Spatial and morphologic relationship of the contiguous cranial air space (red) to the skull (white) of WEN. Panels correspond to the (A) ventral, (B) lateral, (C) anterior and (D) dorsal views. Discontinuous cranial air spaces, excluding the laryngeal air space (also in red), are not shown.

Utilizing the convention of Fraser and Purves (1960), the inflated sinus complex was distinguishable as the primary pterygoid sinus, the mesial and optic lobes of the pterygoid sinus and a middle ear complex consisting of the middle, posterior and peribullary sinuses (Fig. 3). The cranial air space was compartmentalized by the nasal plugs dorsally and the contracted palatopharyngeus muscle around the tip of the larynx below. Accessory and vestibular air sacs were not inflated in WEN, but partial inflation of the pre-maxillary air sacs was observed in CIN. Air spaces directly abutted the tympano-periotic complex such that a bone–air interface existed (Fig. 4). Coverage was most complete on the dorsal, medial and posterior surfaces of the tympano-periotic complex, with the dorsal surface being almost completely covered by a layer of air (Fig. 4A,B). Air coverage of the lateral, ventral and anterior surfaces of the bulla was less complete; soft tissue connections are known to occur at these sites.

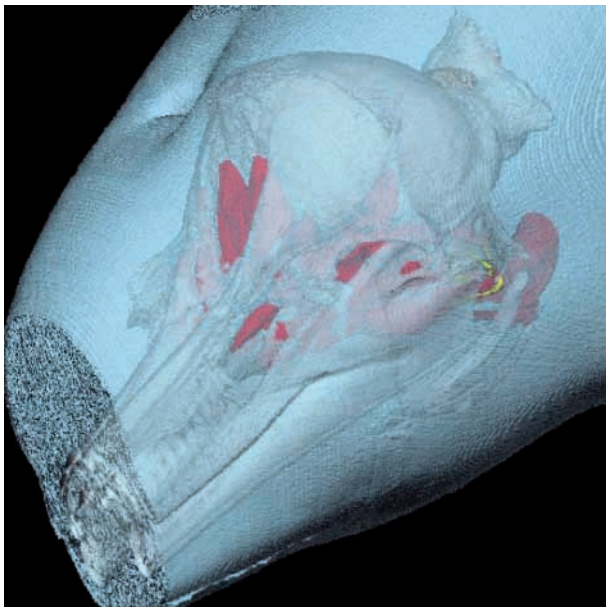

Fig. 2. Spatial and morphologic relationship of the contiguous cranial air space (red) to the skull (white), auditory bulla (yellow), brain and spinal cord (light brown) and other soft tissues (blue) of the head of the bottlenose dolphin WEN. Discontinuous cranial air spaces, excluding the laryngeal air space, are not shown.

SPECT

Uptake of ^{99m}Tc-bicisate is indicative of regional blood

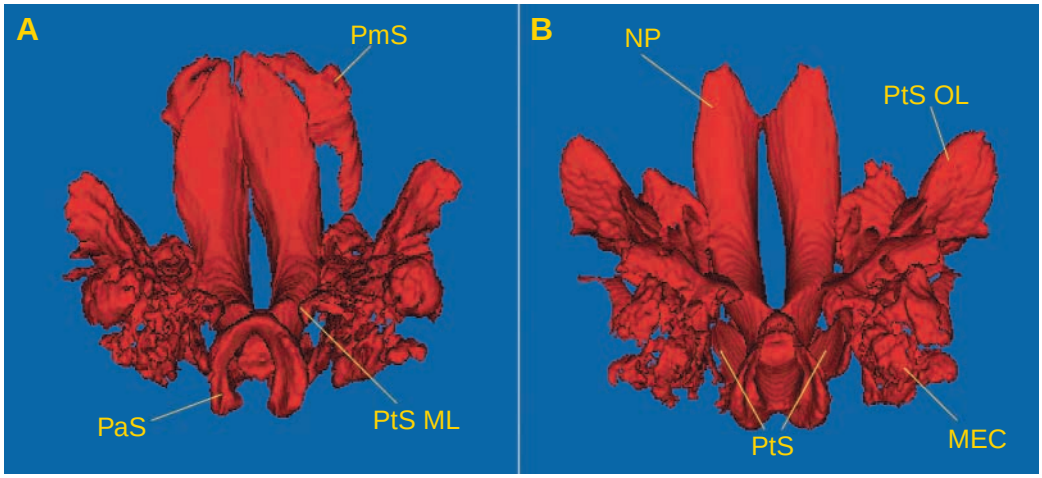

Fig. 3. Regional identification of the bony nasal passages and sinus complex (according to Fraser and Purves, 1960) in (A) CIN and (B) WEN. The objects in the figure represent the actual air space not the tissue boundaries of the air space. Compartmentalization of the cranial air space results from the constriction of the nasal plug and the palatopharyngeus muscle. NP, nasal passages; PtS, primary pterygoid sinus; PtS OL, optic lobe of the pterygoid sinus; PtS ML, mesial lobe of the pterygoid sinus; MEC, middle ear complex; PmS, pre-maxillary sac; PaS, constriction of the palatopharyngeal sphincter.

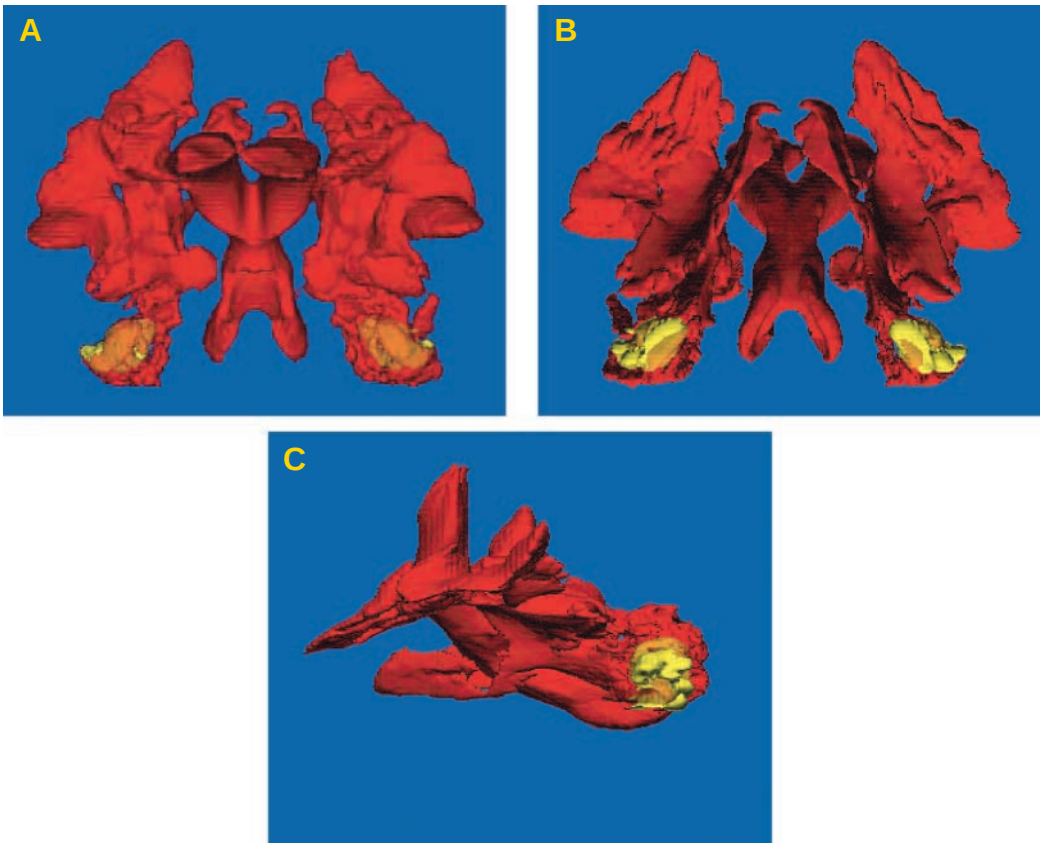

Fig. 4. Relationship of middle ear complex and other cranial air spaces (red) to the tympano-periotic complex (yellow) in the dolphin WEN. Views are from the (A) dorsal, (B) ventral and (C) lateral perspectives.

flow, and substantial uptake was noted in the brain, melon and posterior region of the lower jaw, suggesting extensive blood flow within these tissues (Fig. 5). Uptake by the melon was greater than four times that of the blubber and surrounding soft tissues (based upon the number of counts recorded at each site), and the maximum intensity within the melon was 196% that of the maximum intensity measured in the brain. (Caution must be exercised when interpreting the difference in intensity

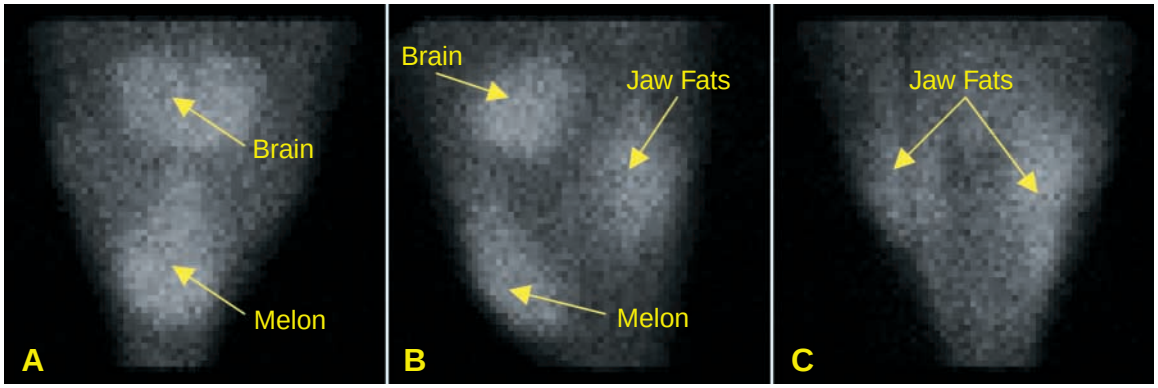

Fig. 5. Multiple views of regional ^{99m}Tc-bicisate uptake in the dolphin WEN. The degree of uptake is directly related to the intensity of the region. Greatest uptake occurs in the brain, melon and bilaterally in the posterior region of the lower jaw. (A) Dorsally, uptake in the brain and melon are apparent. (B) Laterally, the melon (left), brain (top-center) and posterior region of the lower jaw (right) are apparent. (C) Ventrally, uptake in the lower jaw is notable bilaterally.

between the melon and brain as resulting from greater blood flow in the melon than in the brain. ^{99m}Tc-bicisate is soluble in lipid and it is unknown whether the lipid composition of the melon results in a disproportionate uptake of ^{99m}Tc-bicisate relative to the brain for the same rate of blood flow.) Distribution of ligand in the region of the melon was greatest in the dorsoanterior portion of the melon, forming an almost shield-like vascularization that followed the forehead contour (Fig. 6). The greatest amount of ligand uptake in the dorsal region of the melon was immediately sub-dermal while the greatest uptake in the anterior portion of the melon was approximately 4.5 cm subdermal, posterior to the junction of the forehead and rostrum. This region presumably contains an increase in connective tissue proliferation, as has been observed in other odontocete species (Cranford et al., 1996).

PET

Three PET scans were taken of subject WEN; however, the field of view (FOV) was incapable of capturing both the complete melon and brain within the same scan. The uptake of FDG was demonstratively greater within the brain than in any other tissue whereas little to no uptake of FDG was observed in portions of the melon that were within the scan FOV (Fig. 7). Uptake was observed in the region of the peribullary, middle and posterior sinuses and appeared to be consistent with the passage of neural fibers from the brain to the ears (Fig. 8).

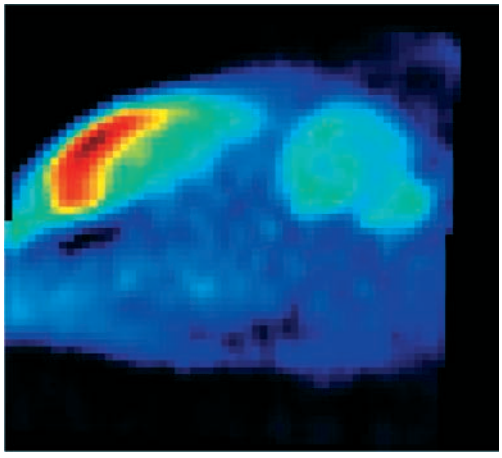

Fig. 6. Sagittal midline view of ^{99m}Tc-bicisate uptake in the melon and brain of the dolphin WEN. Uptake of ^{99m}Tc-bicisate increases as the color scale progresses from blue to red. Greatest uptake occurs in the frontal region of the melon, suggesting that blood flow across the melon is distributed dorsally and anteriorly.

Discussion

The melon is a structure rich in short- and medium-chain fatty acids, particularly isovaleric acid, which is preferentially accumulated relative to its distribution in the blubber (Varanasi and Malins, 1971). The distribution of lipid species throughout the melon is heterogeneous and, because variations in the ratio of wax esters to triacylglycerols alter ultrasonic sound speeds (Varanasi et al., 1975), presumably contributes to the melon's ability to collimate outgoing echolocation clicks. The lower jaws of the dolphin are hollow and thin, with a particularly thin area, known as the 'pan', existing at the posterolateral region of the jaw. Similar to the melon, the mandibular canals are also filled with fat bodies, rich in isovaleric acid, which extend from

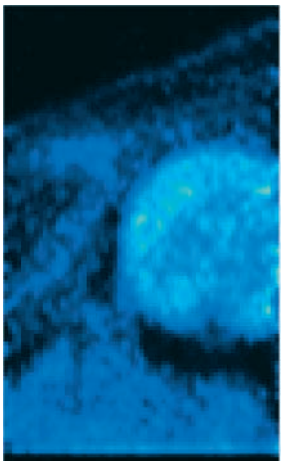

Fig. 7. Sagittal midline section from the dolphin PET series displaying substantial uptake of FDG within the brain and nominal uptake by the melon (lighter, more intense regions correspond to greater uptake). The PET scan image was taken from the dolphin WEN.

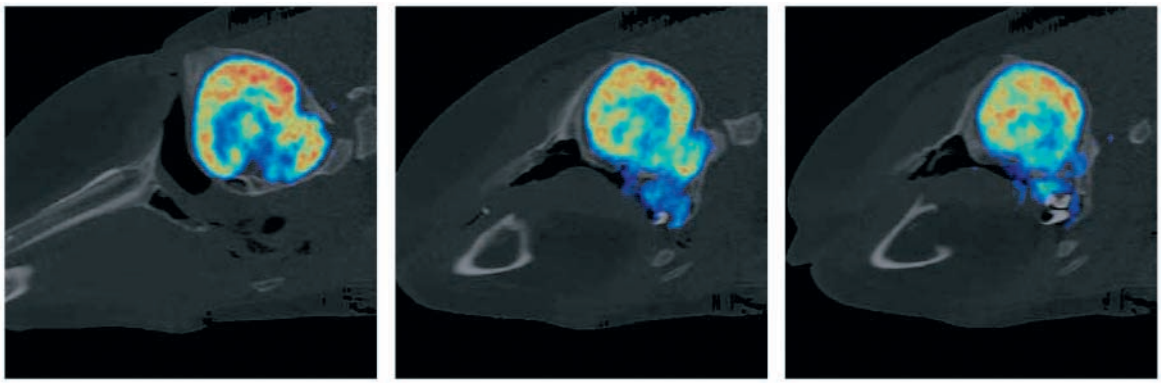

Fig. 8. Representation of co-registered and fused PET and CT scans taken from WEN. Uptake of FDG increases as the color scale progresses from blue to red. The brain is the predominant uptake site of FDG, but distributed uptake occurs throughout the peribullary, middle and posterior sinuses. From left to right, sequential images start with a midsaggital section and progress laterally to the right of the animal. Metabolic activity is notable within the ear cavities lying ventrolateral to the brain.

the posterior of the jaw to make contact with the periotic complex (Varanasi and Malins, 1970b, 1971). The distribution of ^{99m}Tc-bicisate is indicative of perfusion to both the melon and fat bodies in the posterior region of the lower jaw, but lack of uptake of FDG suggests that the melon and fat bodies of the lower posterior jaw are not metabolically active structures. The latter finding is not that surprising given that fat bodies tend to be relatively metabolically inert and that their function as collimator or wave guide is primarily derived from their lipid composition.

It has been proposed that sound refraction can be altered in porpoises by small variations in the chemical composition of the melon, which subsequently impact sound speed through the melon (Varanasi et al., 1975). Variations in ultrasonic speeds of the inner core (1273–1376 m s^{-1}) and outer shell (~1682 m s^{-1}) of the melon of the bottlenose dolphin support this notion (Norris and Harvey, 1974). Similarly, temperature-regulated variations in lipid density should affect the bulk modulus and shear modulus of the melon and fat bodies of the lower jaw as well as the sound speed through these tissues. Sound speed measured through the melon of a deceased dolphin was inversely related to temperature of the melon (Fitzgerald, 1999), and although those sound speed measurements are not likely to be equivalent to measurements recorded in a living animal, the trend will probably be the same.

Variation in blood flow in response to changing water temperatures may stabilize thermal gradients within the lipid complex of the melon and jaw fats by varying heat availability to these regions. Preservation of thermal gradients within the melon appears particularly feasible given the greater distribution of blood flow over the dorsoanterior portion of the melon, a region that is in close contact with water. A temperature change in the outer shell would alter the sound speed gradient between the outer shell and core of the melon and affect the propagation of echolocation clicks. If no mechanism existed to control the temperature-dependent sound speed gradient of the melon, dolphins experiencing variation in water temperatures would also experience a potentially problematic variation in the collimation of outgoing echolocation clicks. Thus, the ability to stabilize the temperature of the melon would be useful in preserving click propagation characteristics and would be advantageous to dolphin species that inhabit environments with seasonal or regional variations in water temperature.

Ligamentous suspension of the bulla provides for acoustic isolation of the ears from the skull (Fraser and Purves, 1960; Ketten and Wartzok, 1990; Reysenbach de Haan, 1956). Similarly, the presence of air around the bulla contributes to acoustic isolation of the ears by providing a sound-reflective barrier between them. The almost complete dorsomedial coverage of the bulla with air should contribute to the animal's ability to differentiate time of arrival differences by impeding conduction through soft tissues that exist between the ears. In combination with other air spaces in the head, this should allow dolphins to capitalize on spectral differences in received signals due to shadowing and may contribute to minimum auditory angular resolution in the vertical and horizontal planes (Popper, 1980; Purves and Van Utrecht, 1963; Renaud and Popper, 1975). Position, geometry and volume of the air spaces within the head of the dolphin are important components of both the sound production and reception process and care should be given to their properties when developing models of biosonar production and hearing in dolphins (e.g. Aroyan, 2001).

Anatomical evidence supports the notion that echolocation clicks are generated by the phonic lips (Cranford et al., 1996; Evans and Prescott, 1962) that lie just superior to the nasal plug. The dorsal and medial air coverage of the bulla, nasal cavity air, the laterally projecting air-filled pterygoid sinuses, and the skull of the dolphin protect the ear from the production of echolocation clicks by acting as acoustic reflectors in the direct path to the ears. However, isolation of the bulla is not complete, as auditory-evoked potentials are elicited in response to a dolphin's own echolocation clicks and have been elicited by transmitting synthetic clicks into the melon of a dolphin

(Bullock and Ridgway, 1972; Supin et al., 2003). For projected clicks, the magnitude of the evoked response is ~20 dB less than that obtained by projecting a click through the lower jaw, which is commonly believed to be the primary receive channel for echoes returning from objects ensonified by a dolphin's biosonar pulses (Brill, 1991; McCormick et al., 1970).

As depth of diving increases, the increasing hydrostatic pressure diminishes the inspired air volume in accordance with Boyle's Law. Thus, air within the cranial air spaces will reduce in volume with increasing depth of diving (Ridgway et al., 1969). The internal carotid artery of *T. truncatus* (and other delphinoids) runs into the middle ear and terminates in the corpus cavernosum carotidis, which is thought to be an erectile tissue (Purves, 1966; Ridgway, 1968). Distension of the corpus cavernosum presumably occurs during diving and reduces the air volume of the sinus space. Purves and Van Utrecht (1963) found that a thin layer of crystallized salt existed around the ossicles of demineralized specimens of *T. truncatus*, even though the corpus cavernosum was apparently engorged to its fullest extent. It therefore appears that, at full distension, the corpus cavernosum and peribullar plexus surrounding the middle ear permit the presence of a thin layer of air. Functionally, this would maintain acoustic isolation of the ears at depth. Additionally, some amount of air may be required to permit mechanical motion of ear components (e.g. round window movement; McCormick et al., 1970).

The nasal passages imaged in the dolphins were compartmentalized by closure of the nasal plug dorsally and constriction of the palatopharyngeus around the tip of the larynx below. The nasal passages are connected to the air sinuses of the head *via* the Eustachian tube. This air is required to drive the pneumatic click source through pressurization of the nasal cavity (Ridgway et al., 1980). While diving, there is an approximate 0.1 MPa increase in pressure for every 10 m that the dolphin dives, and the volume of air within the sinus and nasal air space will decline in proportion to increasing air pressure. Volume reductions in this air space should impact the ability to generate echolocation pulses, thus requiring a mechanism to replenish the air volume and ensure that a pressure differential across the phonic lips can be maintained. Under diving conditions, the palatopharyngeus may mediate exchange between air in the nasal passages and sinuses and air in the lung (Ridgway et al., 1980). Lung collapse obviates alveolar gas exchange at ~70 m depth (Ridgway and Howard, 1979), but movement of air from the lung, bronchi and trachea into the nasal passages and sinus cavities may compensate for a reduction in air volume within those anatomical spaces.

Given that a critical volume of air is likely to be required for click and whistle production and for acoustic isolation of the ears, a theoretical maximum dive depth at which echolocation pulse generation and hearing capability are maintained relative to near-surface functionality can be predicted. Lung volumes between 7 and 11 liters have been estimated for the bottlenose dolphin (Ridgway et al., 1969). Assuming a lung volume of 9 liters, and using the calculated air volume of the sinuses and nasal passages within the dolphin WEN, a maximum dive depth at which both echolocation and hearing capabilities are preserved relative to near-surface functionality can be estimated through the application of Boyle's Law. Further assuming that the nominal amount of air required to preserve echolocation and hearing functionality is equivalent to the volume of air measured in the sinuses and nasal passages at the surface, the maximum depth at which functionality is preserved in the dolphin WEN is calculated to be ~236 m, or 2.5 MPa of pressure. Depending on the technique used, the lung volumes of bottlenose dolphins have been estimated to range from 49 to 71 ml kg^{-1} (Irving et al., 1941; Ridgway et al., 1969) and probably demonstrate an isometric relationship with mass similar to that observed in terrestrial mammals (Schmidt-Nielsen, 1984; Kooyman, 1973). If so, then it seems reasonable that dolphins with larger masses would have a greater depth of diving at which echolocation remains possible, providing them with potential advantages to foraging at depth.

The maximum depth of functional echolocation estimated for WEN is underestimated if the nasal passages are the only cavities requiring air for pressurization of the pneumatic click source, i.e. the sinus space may be diminished to the maximum extent possible through complete distention of the corpus cavernosum and vascular spaces lining the pterygoid sinuses. A reduction in the amount of air required for click generation and hearing will increase the theoretical depth limit at which these functions are preserved. Similarly, if the total lung volume is underestimated, then the maximum depth of normal functionality will also be underestimated. Support for a lesser air volume requirement or greater gas store exists in the observed echolocation of dolphins to depths of up to 300 m (Ridgway et al., 1969). Nevertheless, a maximum depth should exist at which echolocation ceases to be feasible due to a reduction in the volume of gas inspired prior to descent.

Summary

In the present study, recent anatomical and physiological data from bottlenose dolphins that were collected with structural and functional biomedical imaging modalities have provided new insight into the internal anatomy of the head, relative to the cranial air spaces, and identified extensive blood flow in relatively metabolically inert fat bodies. Both of these findings have ramifications to the understanding of dolphin hearing and echolocation. Air in the sinuses and nasal passages is likely to contribute to the hearing capability of the dolphin while simultaneously providing the gas necessary to power the pneumatic source of biosonar pulses. It is speculated that a reduction in the volume of this air that occurs during descent of a dive is replenished by the passage of lung air into the nasal passages *via* the palatopharyngeus muscle. Blood flow over the melon and within the posterior regions of the lower jaw is speculated to function as a thermoregulatory control of lipid density. Thermal regulation of lipid density within both the melon and jaw fats should maintain sound speed gradients within these fatty channels, thus preserving the wave guide action of these sound projection and reception pathways.

The authors would like to thank J. Corbeil and the staff of Vital Imaging and the Department of Nuclear Medicine at the University of California, San Diego Medical Center for their assistance in performing scans. The authors would also like to thank the Biomedical Imaging Resource of the Mayo Clinic, Rochester for their assistance with ANALYZE, and the animal care and training staff of the Space and Naval Warfare Systems Center for their assistance in the training, transport and care of the subjects WEN, CIN and FLP.

References

Aroyan, J. L. (2001). Three-dimensional modeling of hearing in *Delphinus delphis*. *J. Acoust. Soc. Am.* **110**, 3305-3318.

Au, W. W. L. (1993). *The Sonar of Dolphins.* New York: Springer-Verlag.

Brill, R. L. (1991). The effects of attenuating returning echolocation signals at the lower jaw of a dolphin (*Tursiops truncatus*). *J. Acoust. Soc. Am.* **89**, 2851-2857.

Bullock, T. H. and Ridgway, S. H. (1972). Evoked potentials in the central auditory system of alert porpoises to their own and artificial sounds. *J. Neurobiol.* **3**, 79-99.

Cranford, T. W. (1988). Anatomy of acoustic structures in the spinner dolphin forehead as shown by x-ray computed tomography and computer graphics. In *Animal Sonar: Processes and Performance* (ed. P. E. Nachtigall and P. W. B. Moore), pp. 67-77. New York: Plenum Publishing.

Cranford, T. W. (2000). In search of impulse sound sources in odontocetes. In *Hearing by Whales and Dolphins* (ed. W. Au, A. N. Popper and R. R. Fay), pp. 109-156. New York: Springer-Verlag.

Cranford, T. W., Amundin, M. and Norris, K. S. (1996). Functional morphology and homology in the odontocete nasal complex – implications for sound generation. *J. Morphol.* **228**, 223-285.

Dormer, K. J. (1974). *The Mechanism of Sound Production and Measurement of Sound Processing in Delphinid Cetaceans.* Los Angeles: University of California.

Dudok van Heel, W. H. (1962). Sound and cetacea. *Neth. J. Sea Res.* **1**, 407-507.

Evans, W. E. and Prescott, J. H. (1962). Observations of the sound production capabilities of the bottlenosed porpoise: a study of whistles and clicks. *Zoologica* **47**, 121-128.

Fitzgerald, J. W. (1999). The larynx–melon–vestibular lips (LMVL) model of the dolphin sonar. II. The melon beam former. *J. Acoust. Soc. Am.* **105**, 1262-1263.

Fraser, F. C. and Purves, P. E. (1960). Hearing in cetaceans: evolution of the accessory air sacs and the structure and function of the outer and middle ear in recent cetaceans. *Bull. Br. Mus. Nat. His.* **7**, 1-140.

Hunter, J. (1787). Observations on the structure and oeconomy of whales. *Philos. Trans.* **77**, 371-450.

Irving, L., Scholander, P. F. and Grinnell, S. W. (1941). The respiration of the porpoise. *J. Cell. Comp. Physiol.* **17**, 145-168.

Ketten, D. R. (1994). Functional analysis of whale ears: adaptations for underwater hearing. *IEEE Proc. Underwater Acoust.* **1**, 264-270.

Ketten, D. R. (2000). Cetacean ears. In *Hearing by Whales and Dolphins* (ed. W. Au, A. N. Popper and R. R. Fay), pp. 43-108. New York: Springer-Verlag.

Ketten, D. R. and Wartzok, D. (1990). Three-dimensional reconstruction of the dolphin cochlea. In *Sensory Abilities of Cetaceans: Laboratory and Field Evidence* (ed. J. A. Thomas and R. A. Kastelein), pp. 81-105. New York: Plenum Press.

Kooyman, G. L. (1973). Respiratory adaptations in marine mammals. *Am. Zool.* **13**, 457-478.

Mackay, R. S. (1966). Telemetering physiological information from within cetaceans, and the applicability of ultrasound to understanding in vivo structure and performance. In *Whales, Dolphins, and Porpoises* (ed. K. S. Norris), pp. 445-470. Berkeley: University of California Press.

Marino, L., Murphy, T. L., Deweerd, A. L., Morris, J. A., Fobbs, A. J., Humblot, N., Ridgway, S. H. and Johnson, J. I. (2001a). Anatomy and three-dimensional reconstructions of the brain of the white whale (*Delphinapterus leucas*) from magnetic resonance imaging. *Anat. Rec.* **262**, 429-439.

Marino, L., Murphy, T. L., Gozal, L. and Johnson, J. I. (2001b). Magnetic resonance imaging and three-dimensional reconstructions of the brain of a fetal common dolphin, *Delphinus delphis*. *Anat. Embryol.* **203**, 393-402.

Marino, L., Sudheimer, K. D., Murphy, T. L., Davis, K. K., Pabst, D. A., McLellan, W. A., Rilling, J. K. and Johnson, J. I. (2001c). Anatomy and three-dimensional reconstructions of the brain of a bottlenose dolphin (*Tursiops truncatus*) from magnetic resonance images. *Anat. Rec.* **264**, 397-414.

McCormick, J. G., Weaver, E. G., Palin, G. and Ridgway, S. H. (1970). Sound conduction in the dolphin ear. *J. Acoust. Soc. Am.* **48**, 1418-1428.

Nachtigall, P. E., Lemonds, D. W. and Roitblat, H. L. (2000). Psychoacoustic studies of dolphin and whale hearing. In *Hearing by Whales and Dolphins* (ed. W. W. L. Au, A. N. Popper and R. R. Fay), pp. 330-363. New York: Springer-Verlag.

Norris, K. S. and Harvey, G. W. (1974). Sound transmission in the porpoise head. *J. Acoust. Soc. Am.* **56**, 659-664.

Norris, K. W. (1964). Some problems of echolocation in cetaceans. In *Marine Bio-acoustics* (ed. W. N. Tavolga), pp. 317-351. New York: Pergamon Press.

Popper, A. N. (1980). Sound emission and detection by delphinids. In *Cetacean Behavior: Mechanisms and Function* (ed. L. M. Herman), pp. 1-52. New York: John Wiley & Sons.

Purves, P. E. (1966). Anatomy and physiology of the outer and middle ear in cetaceans. In *Whales, Dolphins, and Porpoises* (ed. K. S. Norris), pp. 321-380. Berkeley: University of California Press.

Purves, P. E. and Van Utrecht, W. L. (1963). The anatomy and function of the ear of the bottle-nosed dolphin (*Tursiops truncatus*). *Beaufortia* **9**, 241-256.

Renaud, D. L. and Popper, A. N. (1975). Sound localization by the bottlenose porpoise *Tursiops truncatus*. *J. Exp. Biol.* **63**, 569-585.

Reysenbach de Haan, F. W. (1956). Hearing in whales. *Acta Otolaryngol. Suppl.* **134**, 1-114.

Ridgway, S. H. (1968). The bottlenosed dolphin in biomedical research. In *Methods of Animal Experimentation*, vol. 3 (ed. W. I. Gay), pp. 387-440. New York: Academic Press.

Ridgway, S. H. and Howard, R. (1979). Dolphin lung collapse and intramuscular circulation during free diving: evidence from nitrogen washout. *Science* **206**, 1182-1183.

Ridgway, S. H., Scronce, B. L. and Kanwisher, J. (1969). Respiration and deep diving in the bottlenose porpoise. *Science* **166**, 1651-1654.

Ridgway, S. H., Carder, D. A., Green, R. F., Gaunt, A. S., Gaunt, S. L. L. and Evans, W. E. (1980). Electromyographic and pressure events in the nasolaryngeal system of dolphins during sound production. In *Animal Sonar Systems* (ed. R. G. Busnel and J. F. Fish), pp. 239-250. New York: Plenum Press.

Robb, R. A. (1999). *Biomedical Imaging, Visualization and Analysis*. New York: John Wiley & Sons.

Robb, R. A. and Barillot, C. (1989). Interactive display and analysis of 3-D medical images. *IEEE Trans. Med. Imaging* **8**, 217-226.

Robb, R. A., Hanson, D. P., Karwoski, R. A., Larson, A. G., Wlrkman, E. L. and Stacy, M. C. (1989). ANALYZE: a comprehensive, operator-interactive software package for multidimensional medical image display and analysis. *Comput. Med. Imaging Graph.* **13**, 433-454.

Schmidt-Nielsen, K. (1984). *Scaling, Why is Animal Size so Important?* New York: Cambridge University Press.

Supin, A. Y., Nachtigall, P. E., Pawloski, J. and Au, W. W. L. (2003). Evoked potential recording during echolocation in a false killer whale *Pseudorca crassidens*. *J. Acoust. Soc. Am.* **113**, 2408-2411.

Varanasi, U. and Malins, D. C. (1970a). Ester and ether-linked lipids in the mandibular canal of a porpoise (*Phocoena phocoena*). Occurrence of isovaleric acid in glycerolipids. *Biochemistry* **9**, 4576-4579.

Varanasi, U. and Malins, D. C. (1970b). Unusual wax esters from the mandibular canal of the porpoise (*Tursiops gilli*). *Biochemistry* **9**, 3629-3631.

Varanasi, U. and Malins, D. G. (1971). Unique lipids of the porpoise (*Tursiops gilli*): differences in triacyl glycerols and wax esters of acoustic (mandibular canal and melon) and blubber tissues. *Biochim. Biophys. Acta* **231**, 415-418.

Varanasi, U., Feldman, H. R. and Malins, D. C. (1975). Molecular basis for formation of lipid sound lens in echolocating cetaceans. *Nature* **255**, 340-343.